RSC Advances

PAPER

Cite this: *RSC Adv.*, 2020, **10**, 36713

Multicomponent synthesis of dispiroheterocycles using a magnetically separable and reusable heterogeneous catalyst†

Yogesh Kumar Tailor, Sarita Khandelwal, Kanchan Verma, Ram Gopal and Mahendra Kumar *

Received 2nd August 2020
Accepted 22nd September 2020

DOI: 10.1039/d0ra06676a

rsc.li/rsc-advances

Dispiroheterocycles have been synthesized by pseudo-four component reaction of 6-aminouracil/6-amino-2-thiouracil/2-amino-1,3,4-thiadiazole, *p*-toluidine and isatins in an ethanol–water mixture as solvent using β-cyclodextrin functionalized Fe_3O_4 nanoparticles as a magnetically separable and reusable heterogeneous catalyst. The nanocatalyst was synthesized and characterized by physicochemical characterization including Fourier-transform infrared spectroscopy (FT-IR), scanning electron microscopy (SEM), transmission electron microscopy (TEM), energy-dispersive X-ray spectroscopy (EDX), and X-ray diffraction (XRD).

Introduction

Domino construction of structurally diverse complex molecules avoiding multi-step synthesis and hazardous organic solvents has been a focus of research in view of environmental sustainability and use of synthesized molecules in drug discovery and medicinal chemistry.[1,2] Multicomponent reactions (MCRs) have emerged as significant and sustainable synthetic strategies in view of their exceptional synthetic efficiency and high atom economy to construct structurally diverse and highly functionalized complex drug-like molecules. Multi-component reactions involve the formation of multiple bonds in one-pot operation without isolating the intermediates and without changing the reaction conditions. Moreover, these reactions avoid difficult purification steps and conserve both solvents and reagents. The synthetic efficiency and operational simplicity of multicomponent reactions make them cost effective, time efficient and eco-friendly in comparison to conventional multistep synthesis.[3–8].

Supramolecular catalysis is also an emerging field in chemical research in which the host–guest interactions can regulate the specific reaction.[9] β-Cyclodextrin, macrocyclic oligosaccharide, is an interesting supramolecular catalyst because of being economical, nontoxic, biodegradable, and easily recoverable and reusable.[10,11] β-Cyclodextrin with its hydrophobic cavities binds substrates *via* non-covalent interactions and catalyzes chemical reactions with high selectivity.[12,13]

The use of nanostructured heterogeneous catalysts in organic transformations has recently attracted attention in view of their catalytic efficiency, selectivity and recyclability.[14,15] The magnetic nanocomposites not only catalyze the reactions on their own, but also serve as an effective support for immobilization of active catalyst and facilitate magnetic separation of catalyst for their recovery and reusability.[16] β-Cyclodextrin forms self assembled composite with iron oxide surface by forming hydrogen bonds through hydroxyl groups of β-cyclodextrin. The use of β-cyclodextrin increases the solubility of the catalyst because of the large number of hydroxyl groups around the rim of the cavity, thus acts as a stabilizing agent and can catalyze chemical reaction with high selectivity.[17,18]

The use of water as a solvent for organic synthesis has provided more economic and sustainable synthetic routes.[19,20] Although most of the organic substrates exhibit low solubility in water, β-cyclodextrin nanocomposite consisting of a hydrophobic cavity solubilizes the organic substances in water with the formation of inclusion complex.[21–24] Moreover, the non-covalent interactions are responsible for the lowering of energy barrier and for stabilization of intermediate. The presence of water content in solvent facilitates the reaction probably through non-covalent interactions.[25]

Pyrimido[4,5-*d*]pyrimidines[26] are considered annulated uracils and constitute an important class of biologically significant molecules because of their structural relationship with purine and pteridine heterocyclic systems. The compounds incorporating pyrimidopyrimidinering system have been reported to exhibit diverse activities such as antimicrobial,[27] hepatoprotective,[28] antiviral,[28] antibacterial,[28] anticancer activity[29] and anti-HIV activity.[30]

1,3,5-Triazine is also used as lead structure and incorporated in natural and synthetic pharmaceuticals. 1,3,5-Triazines exhibit

Department of Chemistry, University of Rajasthan, Jaipur, India. E-mail: mahendrakpathak@gmail.com; Tel: +91-0141-2702720

† Electronic supplementary information (ESI) available. See DOI: 10.1039/d0ra06676a

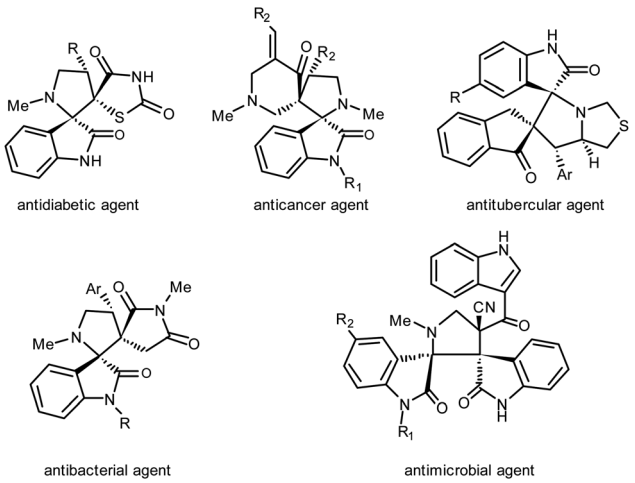

Fig. 1 Representative bioactive dispiroheterocycles.

broad spectrum of activities such as anti-HIV,[31] anticancer,[32,33] antiprotozoal,[34] antimicrobial,[35] antibacterial,[36] antifungal,[37] anti-inflammatory,[38] antimalarials,[39] antitrypanosomal,[40] anti-proliferative,[41] carbonic anhydrase IX inhibitors[42] and diuretic activities.[43]

Dispiroheterocycles represent a class of structurally complex bioactive molecules and incorporated as core units in a number of natural and synthetic pharmaceuticals[44,45] (Fig. 1). In most of the cases as reported in the literature, dispiroheterocycles have been synthesized by [3 + 2] cycloaddition of *in situ* generated azomethine ylides with dipolarophiles.[46–48] But in the present work, we have presented the synthesis of dispiroheterocycles spiroannulated with privileged heterocyclic substructures *via* domino synthetic protocol using β-CD functionalized nano-structured heterogeneous catalyst.

In view of our continuing efforts to develop environmentally sustainable protocol,[49–56] we have presented synthetic protocol to synthesize a library of dispiroheterocycles incorporating unique combination of three or four privileged substructures.

Results and discussion

In the present work, we have synthesized dispiroheterocycles *via* pseudo-four component reaction of 6-aminouracil/6-amino-2-thiouracil/2-amino-1,3,4-thiadiazole, *p*-toluidine and isatins in aqueous-ethanol mixture using β-CD functionalized Fe_3O_4 nanoparticles as magnetically separable and reusable catalyst. Initially, the reaction of 6-aminouracil, *p*-toluidine and isatin

Table 1 Optimization of reaction conditions[a,b]

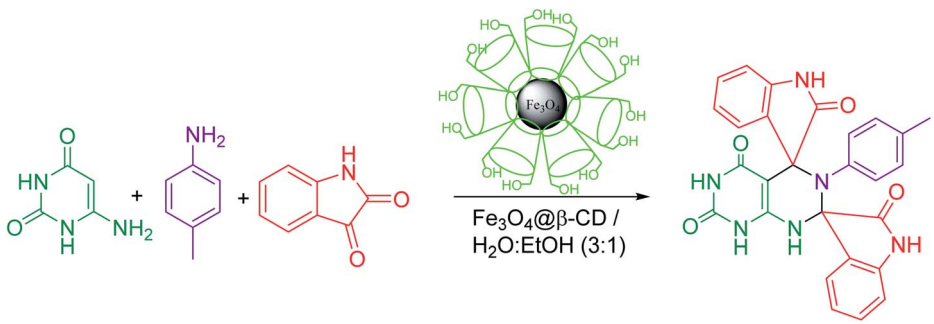

Entry	Catalysts	Solvent[c]	Temperature	Time	Yield[d] (%)
1	Catalyst free	Solvent free	rt	10 h	—
2	Catalyst free	Ethanol	Reflux	8h	Trace
3	Catalyst free	Water	Reflux	8h	Trace
4	$FeCl_3$ (10 mol%)	Ethanol	Reflux	5 h	40
5	$InCl_3$ (10 mol%)	Ethanol	Reflux	5 h	53
6	ZnO NPs (10 mol%)	Ethanol	Reflux	3h	58
7	ZrO_2 NPs (10 mol%)	Ethanol	Reflux	3h	64
8	Fe_3O_4 NPs (10 mol%)	Ethanol	Reflux	3 h	70
9	β-CD	Ethanol	Reflux	2 h	62
10	β-CD	Water	Reflux	2 h	70
11	β-CD	Water : ethanol (3 : 1)	Reflux	2 h	74
12	Fe_3O_4@β-CD NPs (30 mg)	Ethanol	Reflux	80 min	79
13	Fe_3O_4@β-CD NPs (30 mg)	Water	Reflux	60 min	85
14	**Fe_3O_4@β-CDNPs (30 mg)**	**Water : ethanol (3 : 1)**	**Reflux**	**45 min**	**92**
15	Fe_3O_4@β-CD NPs (25 mg)	Water : ethanol (3 : 1)	Reflux	45 min	90
16	Fe_3O_4@β-CD NPs (20 mg)	Water : ethanol (3 : 1)	Reflux	45 min	89

[a] Bold row indicates the optimized reaction conditions. [b] 6-Aminouracil (1 mmol), *p*-toluidine (1 mmol) and isatin (2 mmol), were refluxed with stirring. [c] Solvents (2.0 mL). [d] Isolated yield after purification.

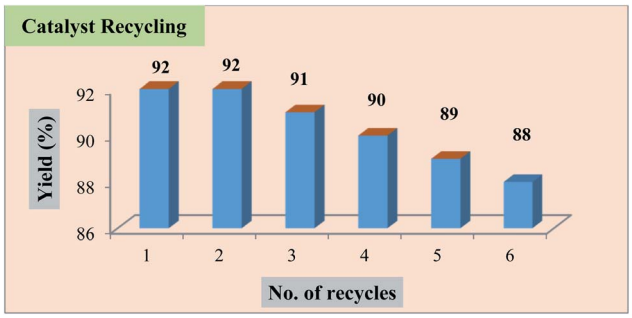

Fig. 2 Recyclability and reusability of Fe_3O_4@β-CD NPs.

was selected as a model reaction to optimize the reaction conditions and to explore the feasibility of the present synthetic strategy (Table 1).

It was observed that the reaction could not provide the desired product when performed in solvent and catalyst free conditions even after continuous stirring the reactants at room temperature for 10 h (Table 1, entry 1). But when the reaction was carried out in ethanol and water separately as solvents in the absence of a catalyst, trace amount of the product was obtained (Table 1, entries 2 and 3). Thus, it was evident from these observations that the reaction required suitable catalyst to provide the desired product. The reaction was also performed with Lewis acid catalysts; $FeCl_3$ and $InCl_3$, using ethanol as solvent, but both the Lewis acid catalysts provided the product in low yield (Table 1, entries 4 and 5). The reaction was also performed with three nano-catalysts; ZnO, ZrO_2 and Fe_3O_4 in ethanol as solvent, the use of catalyst Fe_3O_4 NPs provided comparatively better yield (Table 1, entries 6–8). The reaction conditions were also optimized by performing the reaction with organocatalyst β-cyclodextrin using ethanol, water, and water–ethanol mixture as solvents and observed that β-cyclodextrin as catalyst with water : ethanol (3 : 1) mixture as solvent provided better results (Table 1, entries 9–11). The model reaction was also evaluated in the presence of Fe_3O_4@β-CD nanoparticles as catalyst using separately three solvents (Table 1, entries 12–14) and observed that the reaction with the use of Fe_3O_4@β-CD nanoparticles as catalyst in water : ethanol (3 : 1) mixture as solvent provided maximum yield of the product in shorter reaction time. Thus, the excess of water content in solvent (3 : 1) up to some extent facilitates the reaction probably through non-covalent interactions, hydrogen bonding. Therefore, on the basis of these observations, Fe_3O_4@β-CD nanoparticles as catalyst exhibited excellent catalytic activity in terms of product yield and duration of the reaction. The functionalization of Fe_3O_4 nanoparticles with β-CD increases catalytic activity and facilitates the reaction to a greater extent to provide the product in excellent yield.

The influence of catalyst loading on the yield of the product was also evaluated with the loading amounts of the catalyst. With these observations, it was inferred that 30 mg of Fe_3O_4@β-CD nanoparticles provided the maximum yield of the product in shorter conversion time (Table 1, entries 14–16). After completion of the reaction, the catalyst was recovered by using external magnetic field. The recovered catalyst was washed well with

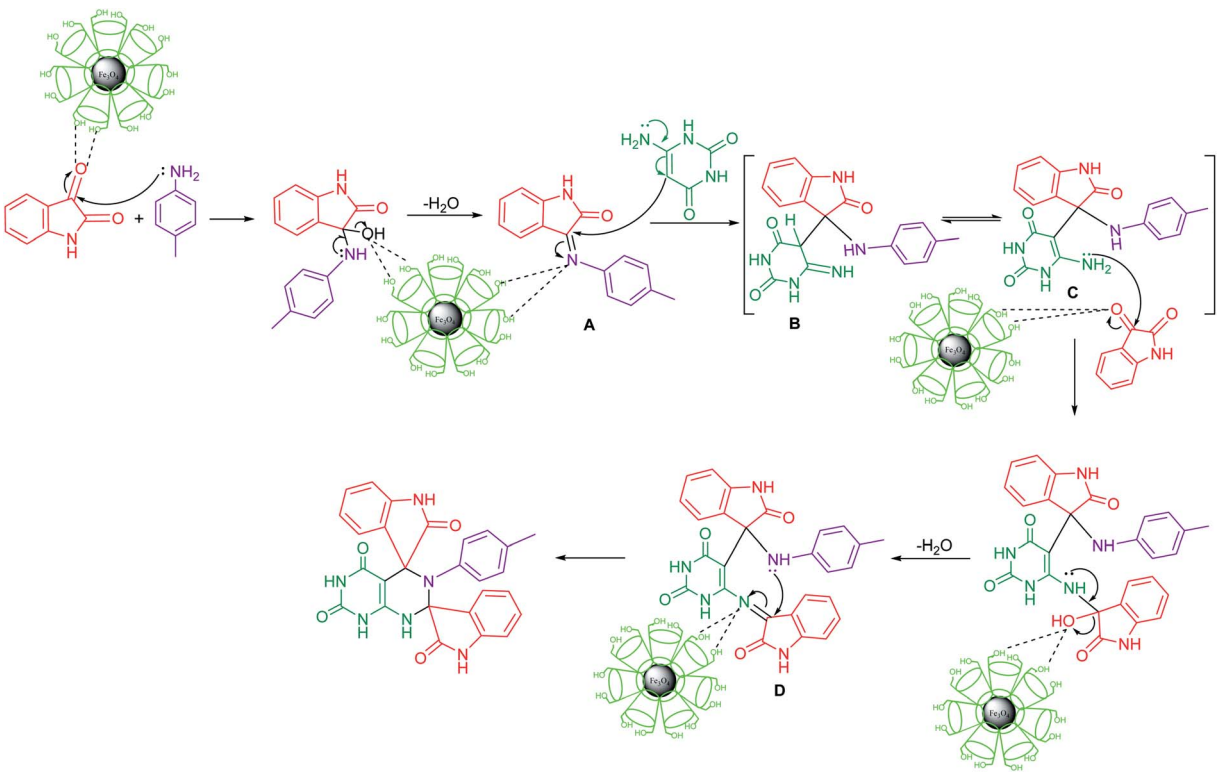

Scheme 1 Proposed mechanism.

ethanol, dried at room temperature and reused for subsequent reaction cycles without an appreciable loss in catalytic activity (Fig. 2).

Under the optimized reaction conditions, the reaction was extended with 6-aminouracil/6-amino-2-thiouracil/2-amino-1,3,4-thiadiazol/2-amino-1,3,4-thiadiazole, isatins and *p*-toluidine to synthesize a library of dispiroheterocycles with a view to explore the feasibility and scope of the present synthetic protocol. The synthesized dispiroheterocycles are presented in Tables 2–4.

Mechanism

The reaction mechanisms of the multicomponent reactions cannot be investigated by the usual methods. However, some essential mechanistic information on multicomponent reaction may be obtained only from the combinations of several

Table 2 Synthesis of dispiroheterocycles spiroannulated with pyrimido[4,5-*d*]pyrimidine

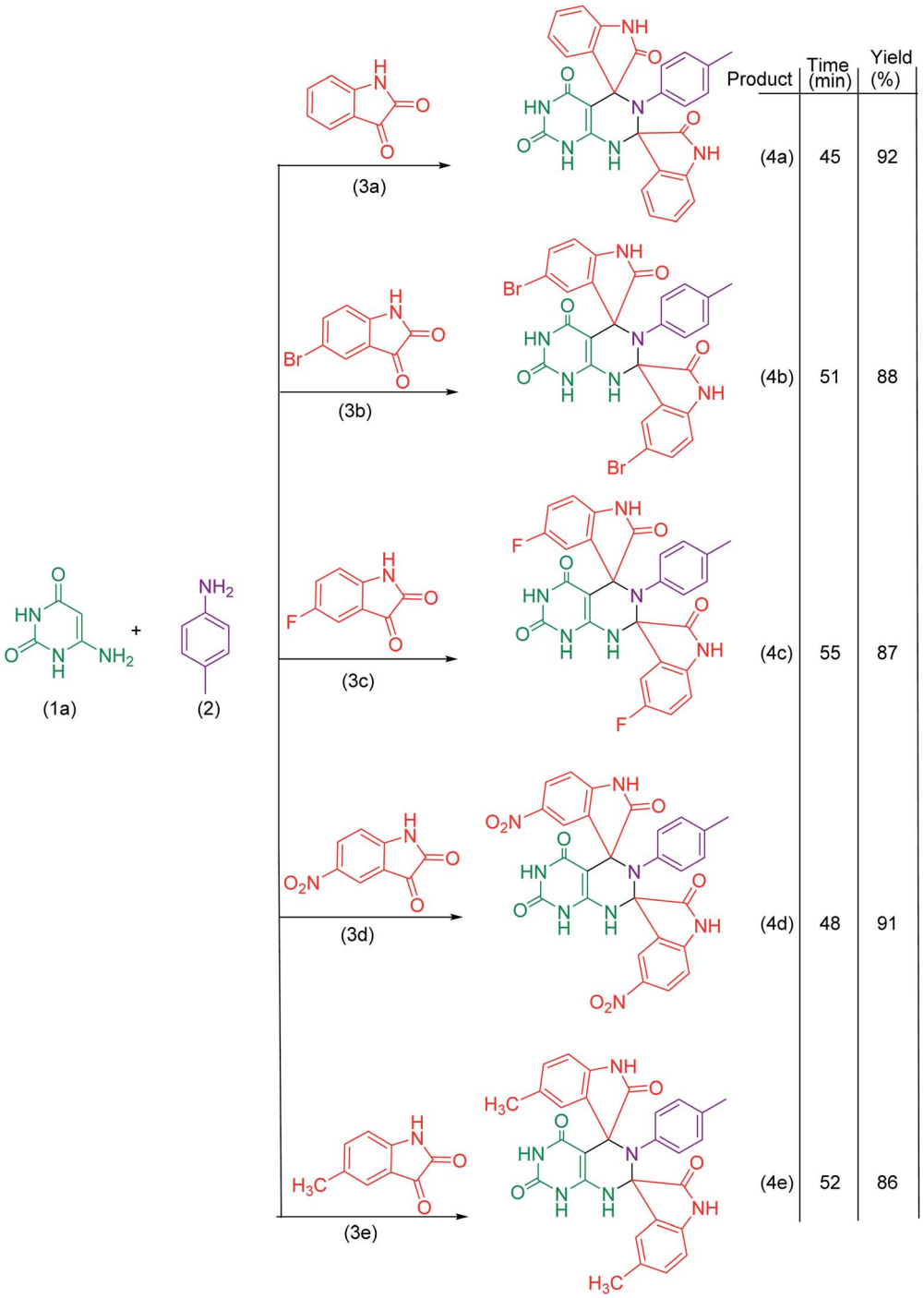

Product	Time (min)	Yield (%)
(4a)	45	92
(4b)	51	88
(4c)	55	87
(4d)	48	91
(4e)	52	86

Table 3 Synthesis of dispiroheterocycles spiroannulated with thioxopyrimido[4,5-*d*]pyrimidine

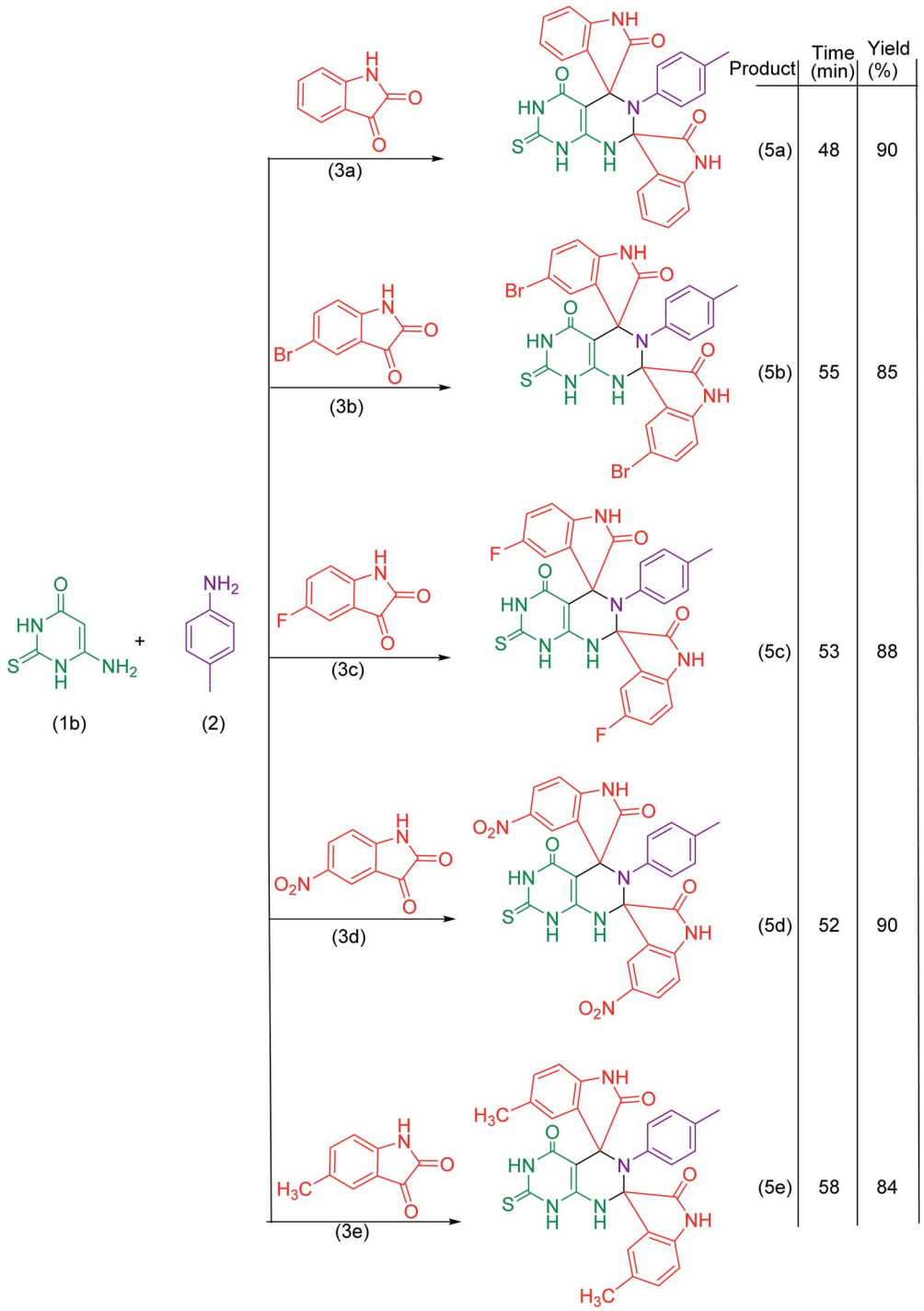

methods, but not all of the usual detailed information can be expected for transformation. The possible and accepted mechanism of multicomponent reaction may be determined on the basis of the noncovalent interactions between *in situ* generated preferential intermediate and catalytic framework.[25]

A plausible mechanism of the reaction is presented in (Scheme 1). The reaction is considered to proceed with the nucleophilic attack of amino group of amine on carbonyl carbon of isatin with the formation of imine intermediate A involving nucleophilic addition–elimination reaction. In the next step, the nucleophilic attack of enamino carbon of 6-aminouracil occurs on the carbon of C=N group with the formation of intermediate **B** which is in equilibrium with more stabilized enamine intermediate **C** through noncovalent interactions with

Table 4 Synthesis of dispiroheterocycles spiroannulated with [1,3,4]thiadiazolo[3,2-*a*][1,3,5]triazine

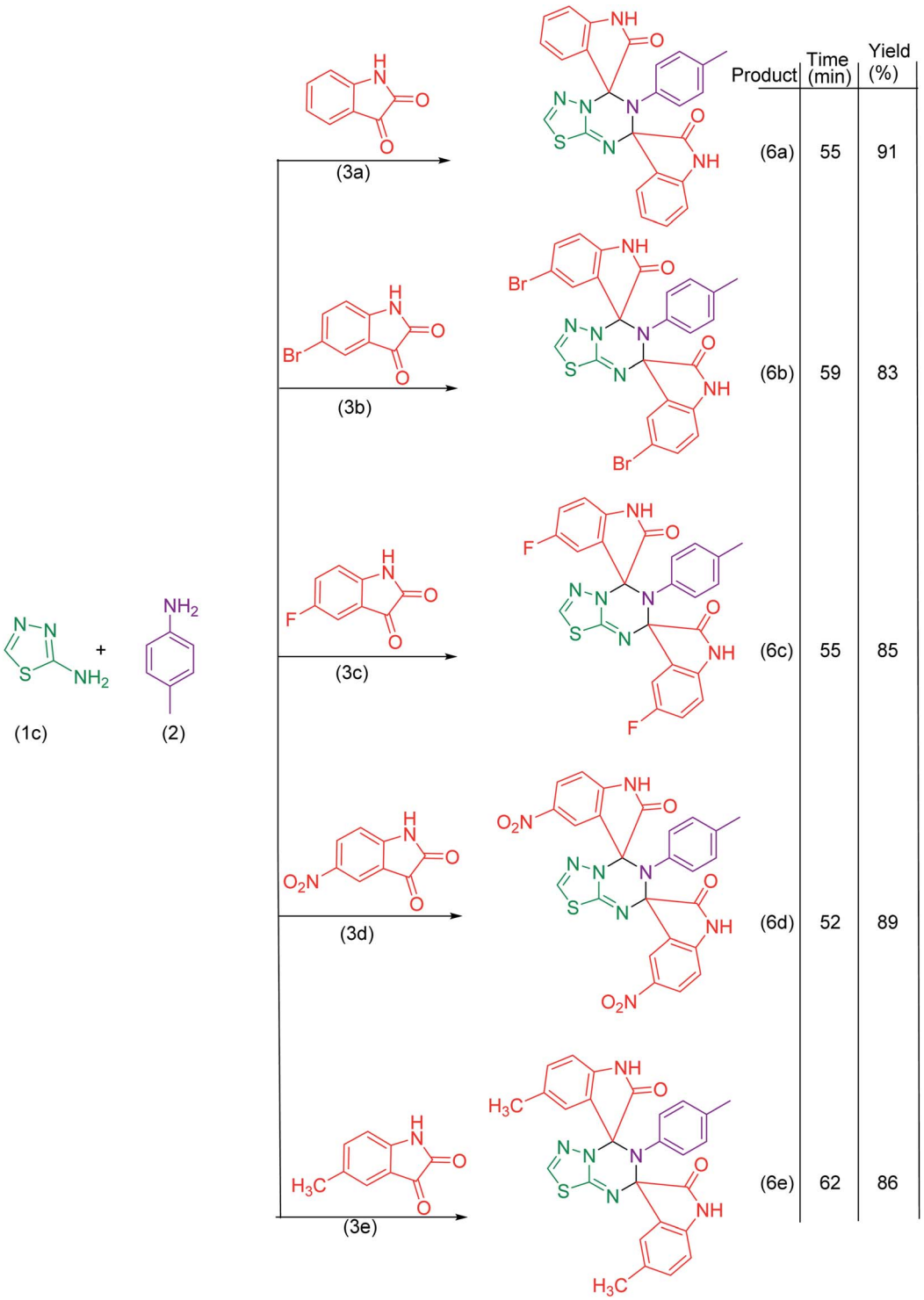

catalyst framework. The stabilization of the intermediate facilitates the reaction to proceed in the forward direction. Next step of the reaction involves nucleophilic attack of amino group of enamine intermediate on carbonyl carbon of second molecule of isatin followed by dehydration and subsequent intramolecular cycloaddition of –NH group to the C=N group of the resulting intermediate **D** to afford the final product. The required organization of the reagents in any catalyzed reaction is influenced by intermolecular noncovalent interactions. These noncovalent forces are in fact responsible for the lowering of energetic barriers and thus stabilization of transition states. In the present domino sequential reaction, the competitive

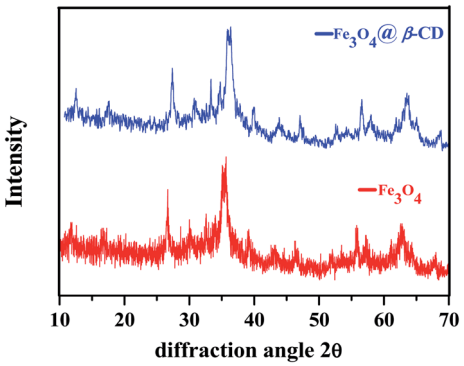

Fig. 3 The XRD patterns of Fe_3O_4 and Fe_3O_4@β-CD.

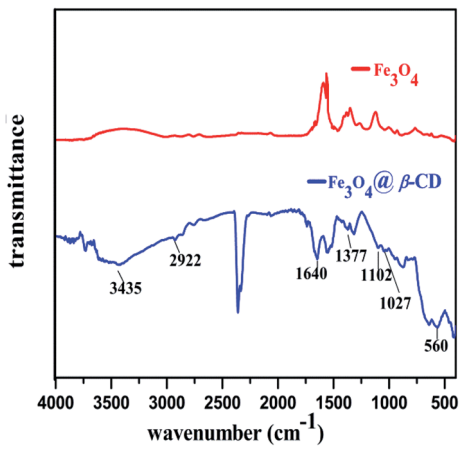

Fig. 4 The FT-IR spectra of Fe_3O_4 and Fe_3O_4@β-CD.

mechanism of the reaction is not possible whatever be the sequence of the reaction of the reagents with catalyst framework. In the multicomponent reaction, all the changes including generation of intermediates occur *in situ* and the intermediates are stabilized through noncovalent interactions with catalytic framework. Thus, the key role of the noncovalent interactions is the stabilization of the intermediates generated *in situ* during the reaction.

Experimental

General procedure

The melting points of synthesized dispiroheterocycles were determined on electric melting point apparatus and are uncorrected. 2-Amino-1,3,4-thiadiazole/6-aminouracil/6-amino-2-thiouracil, isatins, *p*-toluidine, salts of iron(II) chloride, iron(III) chloride and β-cyclodextrin were purchased from the commercial sources and used as such in the reactions. The purity of all the synthesized compounds was checked by TLC and their ^{1}H NMR and ^{13}C NMR were recorded on JEOL 400 MHz and 100 MHz NMR spectrometer, respectively. The nanocatalyst was synthesized and characterized by physicochemical characterization tools. FT-IR spectra of catalyst was obtained over the region 400–4000 cm^{-1} with a Nicolet IR 100 FT-IR with spectroscopic grade KBr. XRD patterns were recorded on a PAN analytical make X'Pert PRO MPD diffractometer (model 3040). SEM was performed on Carl-Zeiss (30 keV) make and model EVO 18. TEM and EDX were carried out on XFlesh CTI 30 (200 keV) Bruker.

Typical procedure for synthesis of Fe_3O_4@β-CD

β-Cyclodextrin functionalized Fe_3O_4 nanoparticles were successfully synthesized by reported method[18] and characterized by physicochemical characterization including Fourier-transform infrared spectroscopy (FT-IR), scanning electron microscopy (SEM), transmission electron microscopy (TEM), energy-dispersive X-ray spectroscopy (EDX), and X-ray diffraction (XRD).

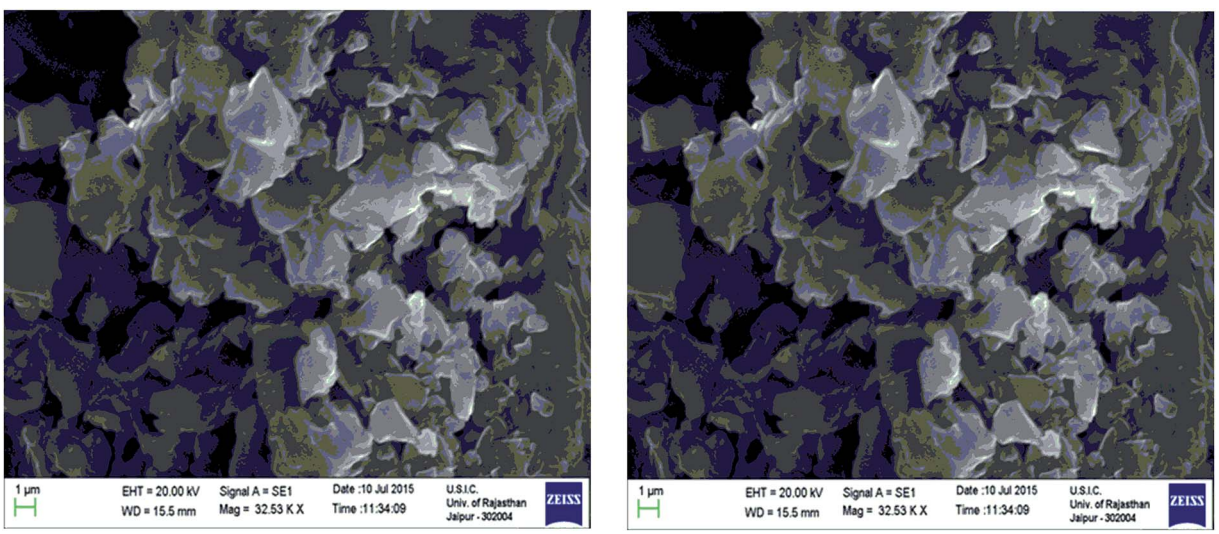

Fig. 5 (a) The SEM images of Fe_3O_4, (b) the SEM images of Fe_3O_4@β-CD.

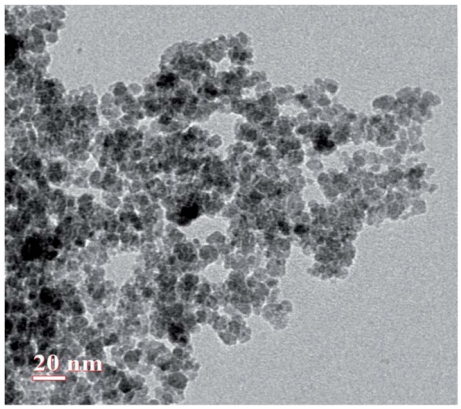

Fig. 6 The TEM image of Fe_3O_4@β-CD.

The XRD patterns of Fe_3O_4 and Fe_3O_4@β-CD are presented in (Fig. 3). The comparison with standard data (PDF #89-4319) indicated the formation of cubic phase. Diffraction peaks of Fe_3O_4 in synthesized Fe_3O_4@β-CD indicate that the crystalline structure of the magnetite is effectively sustained. In addition, some characteristic peaks at 2θ = 27.29, 30.70, 36.25, 47.04, 56.70 63.54 were attributed to XRD spectra of Fe_3O_4 and Fe_3O_4@β-CD which strongly confirmed the structure of Fe_3O_4 after encapsulation. The crystallite size of Fe_3O_4 and Fe_3O_4@β-CD were calculated to be around ~10 nm and ~12 nm, respectively by applying the Scherer equation, based on theoretical calculation of XRD spectrum.

The FT-IR spectra of Fe_3O_4 and Fe_3O_4@β-CD are presented in (Fig. 4). The functionalization of Fe_3O_4 with β-CD was proved by comparing FT-IR spectra of Fe_3O_4 and Fe_3O_4@β-CD. The absorption bands around 3435 cm^{-1} were assigned to the vibrations of C–O–H and Fe–O–H bonds. The characteristic peaks at 2922 cm^{-1} and 1377 cm^{-1} were attributed to the vibrations of aliphatic C–H bond in β-CD associated to Fe_3O_4. The absorption band observed at 1028 cm^{-1} was assigned to the C–O stretching modes of β-CD. The absorption band appeared around 560 cm^{-1} is attributed to the Fe–O bond.

The scanning electron microscopy (SEM) images of Fe_3O_4 and Fe_3O_4@β-CD shown in Fig. 5(a) and (b) indicate the agglomerated nanoflakes morphology, constituted by nano-sized crystallites. The TEM image of Fe_3O_4@β-CD indicates the agglomerated spherical morphology. The average size of the nanoparticles was found to be around 8 nm (Fig. 6). The EDX results indicate the presence of Fe, O and C in Fe_3O_4@β-CD (Fig. 7).

Typical procedure for synthesis of dispiroheterocycles

A mixture of 6-aminouracil/6-amino-2-thiouracil/2-amino-1,3,4-thiadiazol (1 mmol), *p*-toluidine (1 mmol), isatin (2 mmol) and

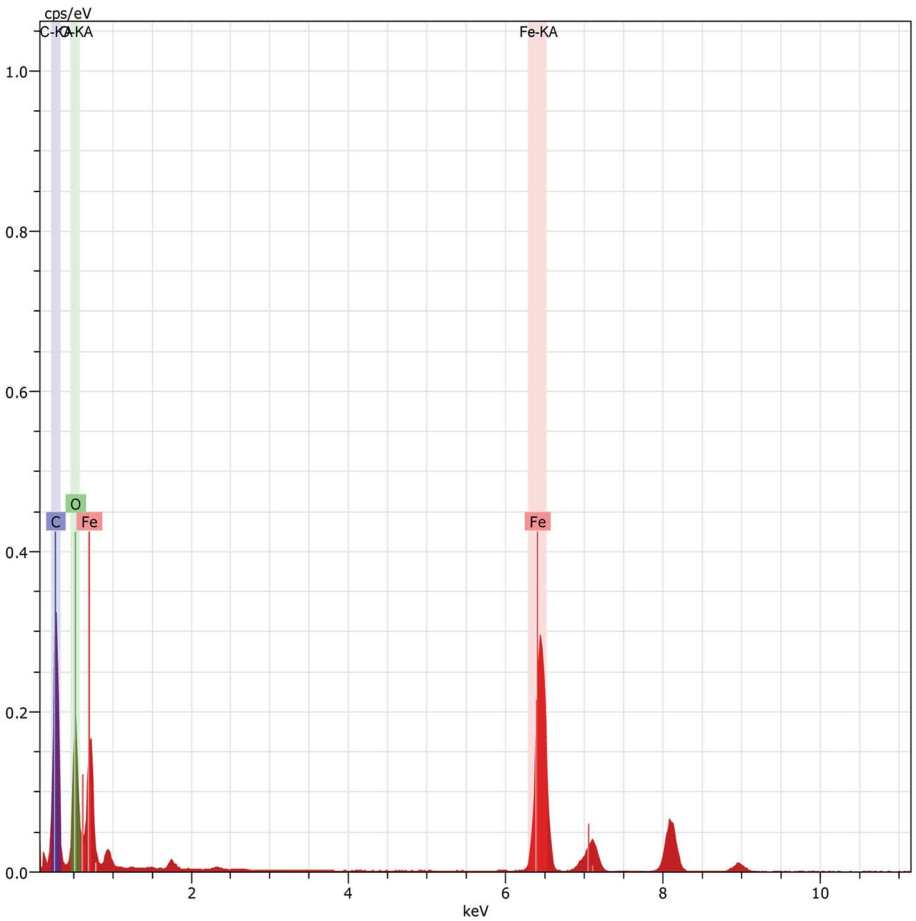

Fig. 7 EDX analysis of the Fe_3O_4@β-CD.

Fe_3O_4@β-cyclodextrin nanoparticles as catalyst (30 mg) in 2.0 mL aqueous ethanol (water : ethanol v/v/3 : 1) was refluxed with stirring for about 45 min to 62 min. The progress of the reaction was monitored by TLC with time ranging from 40–70 min. After completion of the reaction, ethanol was added to the reaction mixture and the catalyst was removed by an external magnet, washed well with ethanol and dried at room temperature and reused for subsequent reaction cycles. The synthesized compounds were purified by recrystallization from absolute ethanol without using column chromatography.

Conclusion

In conclusion, we have presented an efficient and sustainable synthetic protocol to synthesize dispiroheterocycles using β-CD functionalized Fe_3O_4 nanoparticles as magnetically separable and reusable heterogeneous catalyst. The functionalization of Fe_3O_4 nanoparticles with β-cyclodextrin enhanced catalytic efficiency and facilitated the reaction with excellent yields of the reaction products. The sustainability of the catalyst has been demonstrated by its reuse for subsequent reaction cycles without an appreciable loss in its catalytic activity. The present synthetic protocol will provide an environmentally sustainable and economically viable synthetic methodology to access a library of drug-like small molecules with molecular complexity for their use in drug discovery research and pharmaceutical chemistry.

Conflicts of interest

There are no conflicts to declare.

Acknowledgements

We gratefully acknowledge UGC New Delhi for the award of Research Fellowship (SRF) to Kanchan Verma. Head, Department of Chemistry is acknowledged for providing lab and instrumental facilities in the department.

References

1 A. Dömling, W. Wang and K. Wang, *J. Chem. Rev.*, 2012, **112**, 3083–3135.
2 H. Pellissier, *Org. Prep. Proced. Int.*, 2019, **51**, 311–344.
3 I. A. Ibarra, A. Islas-Jácome and E. González-Zamora, *Org. Biomol. Chem.*, 2018, **16**, 1402–1418.
4 L. Wu, S. Yan, W. Wang and Y. Li, *Res. Chem. Intermed.*, 2020, **46**, 4311–4322.
5 H. T. Nguyen, V. A. Truong and P. H. Tran, *RSC Adv.*, 2020, **10**, 25358–25363.
6 H. G. O. Alvim, J. R. Correa, J. A. F. Assumpção, W. A. da Silva, M. O. Rodrigues, J. L. de Macedo, M. Fioramonte, F. C. Gozzo, C. C. Gatto and B. A. D. Neto, *J. Org. Chem.*, 2018, **83**, 4044–4053.
7 S. Zhi, X. Ma and W. Zhang, *Org. Biomol. Chem.*, 2019, **17**, 7632–7650.
8 L. Zeng, B. Huang, Y. Shen and S. Cui, *Org. Lett.*, 2018, **20**, 3460–3464.
9 F. Huang and E. V. Anslyn, *Chem. Rev.*, 2015, **115**, 6999–7000.
10 M. De Rosa, P. La Manna, C. Talotta, A. Soriente, C. Gaeta and P. Neri, *Front. Chem.*, 2018, **6**, DOI: 10.3389/fchem.2018.00084.
11 D. S. Dalal, D. R. Patil and Y. A. Tayade, *Chem. Rec.*, 2018, **18**, 1560–1582.
12 T. D. Urmode, M. A. Dawange, V. S. Shinde and R. S. Kusurkar, *Tetrahedron*, 2017, **73**, 4348–4354.
13 K. Gong, H. Wang, X. Ren, Y. Wang and J. Chen, *Green Chem.*, 2015, **17**, 3141–3147.
14 L. L. Chng, N. Erathodiyil and J. Y. Ying, *Acc. Chem. Res.*, 2013, **46**, 1825–1837.
15 F. Zaera, *Chem. Soc. Rev.*, 2013, **42**, 2746–2762.
16 E. Abroshan, S. Farhadi and A. Zabardasti, *Sol. Energy Mater. Sol. Cells*, 2018, **178**, 154–163.
17 P. Nariya, M. Das, F. Shukla and S. Thakore, *J. Mol. Liq.*, 2020, **300**, 112279.
18 S. Rostamnia and E. Doustkhah, *J. Magn. Magn. Mater.*, 2015, **386**, 111–116.
19 M.-O. Simon and C.-J. Li, *Chem. Soc. Rev.*, 2012, **41**, 1415–1427.
20 A. Chanda and V. V. Fokin, *Chem. Rev.*, 2009, **109**, 725–748.
21 F. Hapiot, S. Menuel, M. Ferreira, B. Léger, H. Bricout, S. Tilloy and E. Monflier, *ACS Sustainable Chem. Eng.*, 2017, **5**, 3598–3606.
22 K. Kanagaraj and K. Pitchumani, *J. Org. Chem.*, 2013, **78**, 744–751.
23 E. A. Kataev, M. Ramana Reddy, G. Niranjan Reddy, V. H. Reddy, C. Suresh Reddy and B. V. Subba Reddy, *New J. Chem.*, 2016, **40**, 1693–1697.
24 J. Wu, X. Du, J. Ma, Y. Zhang, Q. Shi, L. Luo, B. Song, S. Yang and D. Hu, *Green Chem.*, 2014, **16**, 3210–3217.
25 L. M. Ramos, M. O. Rodrigues and B. A. D. Neto, *Org. Biomol. Chem.*, 2019, **17**, 7260–7269.
26 E. C. Taylor, R. J. Knopf, R. F. Meyer, A. Holmes and M. L. Hoefle, *J. Am. Chem. Soc.*, 1960, **82**, 5711–5718.
27 P. Sharma, N. Rane and V. K. Gurram, *Bioorg. Med. Chem. Lett.*, 2004, **14**, 4185–4190.
28 V. J. Ram, A. Goel, S. Sarkhel and P. R. Maulik, *Bioorg. Med. Chem.*, 2002, **10**, 1275–1280.
29 S. A. Al-Issa, *Saudi Pharm. J.*, 2013, **21**, 305–316.
30 T. Venkatesh, Y. D. Bodke and A. S. J. Rao, *Chem. Data Collect.*, 2020, **25**, 100335.
31 N. Sakakibara, G. Balboni, C. Congiu, V. Onnis, Y. Demizu, T. Misawa, M. Kurihara, Y. Kato, T. Maruyama, M. Toyama, M. Okamoto and M. Baba, *Antiviral Chem. Chemother.*, 2015, **24**, 62–71.
32 S. Cascioferro, B. Parrino, V. Spanò, A. Carbone, A. Montalbano, P. Barraja, P. Diana and G. Cirrincione, *Eur. J. Med. Chem.*, 2017, **142**, 523–549.
33 J. Sonika, J. Pankaj Kumar, S. Shalu, D. Kishore and D. Jaya, *Mini-Rev. Org. Chem.*, 2020, **17**, 1–17.
34 M. L. Stock, S. T. Elazab and W. H. Hsu, *J. Vet. Pharmacol. Ther.*, 2018, **41**, 184–194.

35 H. Liu, S. Long, K. P. Rakesh and G.-F. Zha, *Eur. J. Med. Chem.*, 2020, **185**, 111804.
36 U. Divya, K. Jagdish, K. Komalpreet and J. Palak, *Mini-Rev. Org. Chem.*, 2020, **17**, 1–51.
37 S. Amit, S. Sarbjit and U. Divya, *Curr. Org. Synth.*, 2016, **13**, 484–503.
38 L. Marín-Ocampo, L. A. Veloza, R. Abonia and J. C. Sepúlveda-Arias, *Eur. J. Med. Chem.*, 2019, **162**, 435–447.
39 H. R. Bhat, U. P. Singh, P. Gahtori, S. K. Ghosh, K. Gogoi, A. Prakash and R. K. Singh, *New J. Chem.*, 2013, **37**, 2654–2662.
40 M. Venkatraj, I. G. Salado, J. Heeres, J. Joossens, P. J. Lewi, G. Caljon, L. Maes, P. Van der Veken and K. Augustyns, *Eur. J. Med. Chem.*, 2018, **143**, 306–319.
41 S. Ranjbari, M. Behzadi, S. Sepehri, M. Dadkhah Aseman, A. Jarrahpour, M. Mohkam, Y. Ghasemi, A. Reza Akbarizadeh, S. Kianpour, Z. Atioğlu, N. Özdemir, M. Akkurt, S. Masoud Nabavizadeh and E. Turos, *Bioorg. Med. Chem.*, 2020, **28**, 115408.
42 N. Lolak, S. Akocak, S. Bua and C. T. Supuran, *Bioorg. Chem.*, 2019, **82**, 117–122.
43 M. H. Shah, C. V. Deliwala and U. K. Sheth, *J. Med. Chem.*, 1968, **11**, 1167–1171.
44 C. Bharkavi, S. Vivek Kumar, M. Ashraf Ali, H. Osman, S. Muthusubramanian and S. Perumal, *Bioorg. Med. Chem.*, 2016, **24**, 5873–5883.
45 A. S. Girgis, S. S. Panda, E.-S. M. Shalaby, A. F. Mabied, P. J. Steel, C. D. Hall and A. R. Katritzky, *RSC Adv.*, 2015, **5**, 14780–14787.
46 A. R. Suresh Babu, D. Gavaskar and R. Raghunathan, *Tetrahedron Lett.*, 2012, **53**, 6676–6681.
47 M. Zhang, W. Yang, K. Li, K. Sun, J. Ding, L. Yang and C. Zhu, *Synthesis*, 2019, **51**, 3847–3858.
48 K. Martina, S. Tagliapietra, V. V. Veselov and G. Cravotto, *Front. Chem.*, 2019, **7**, 95.
49 S. Khandelwal, Y. K. Tailor and M. Kumar, *J. Mol. Liq.*, 2016, **215**, 345–386.
50 Y. K. Tailor, S. Khandelwal, Y. Kumari, K. Awasthi and M. Kumar, *RSC Adv.*, 2015, **5**, 46415–46422.
51 E. Rushell, Y. K. Tailor, S. Khandewal, K. Verma, M. Agarwal and M. Kumar, *New J. Chem.*, 2019, **43**, 12462–12467.
52 K. Verma, Y. K. Tailor, S. Khandelwal, E. Rushell, M. Agarwal and M. Kumar, *Mol. Diversity*, 2019, DOI: 10.1007/s11030-019-09999-4.
53 K. Verma, Y. K. Tailor, S. Khandelwal, M. Agarwal, E. Rushell, Y. Kumari, K. Awasthi and M. Kumar, *RSC Adv.*, 2018, **8**, 30430–30440.
54 Y. K. Tailor, S. Khandelwal, K. Verma, R. Gopal and M. Kumar, *ChemistrySelect*, 2017, **2**, 5933–5941.
55 Y. K. Tailor, S. Khandelwal, R. Gopal, E. Rushell, A. Prajapati and M. Kumar, *ChemistrySelect*, 2017, **2**, 11055–11061.
56 S. Khandelwal, Y. K. Tailor, E. Rushell and M. Kumar, in *Green Approaches in Medicinal Chemistry for Sustainable Drug Design*, ed. B. K. Banik, Elsevier, 2020, pp. 245–352, DOI: 10.1016/B978-0-12-817592-7.00009-5.

